Journal of Trace Elements in Medicine and Biology 55 (2019) 1–5

Contents lists available at ScienceDirect

Journal of Trace Elements in Medicine and Biology

journal homepage: www.elsevier.com/locate/jtemb

Complementary techniques (spICP-MS, TEM, and HPLC-ICP-MS) reveal the degradation of 40 nm citrate-stabilized Au nanoparticles in rat liver after intraperitoneal injection

Roberto Álvarez-Fernández García[a], Nerea Fernández-Iglesias[a], Carlos López-Chaves[b], Cristina Sánchez-González[b,*], J. Llopis[b], Maria Montes-Bayón[a], Jörg Bettmer[a,*]

[a] University of Oviedo, Faculty of Chemistry, Dept. of Physical and Analytical Chemistry, C/ Julián Clavería 8, E-33006 Oviedo, Spain
[b] University of Granada, Faculty of Pharmacy, Dept. of Physiology, Campus Cartuja, E-18071 Granada, Spain

ARTICLE INFO

Keywords:
Gold nanoparticles
Single particle ICP-MS
HPLC-ICP-MS
TEM
Rat liver tissues

ABSTRACT

Background: Due to the increased use of engineered nanoparticles (NPs), their tracing in environmental and biological systems is of utmost importance. Besides their accumulation within a biological specimen, little is known about their degradation and transformation into corresponding low-molecular species that might influence any toxicological impact.

Analytical methods: Wistar rats underwent intraperitoneal injections of 40 nm citrate-stabilized gold nanoparticles. Different liver samples were analysed for the occurrence of nanoparticles and potential degradation products by means of spICP-MS, TEM and HPLC-ICP-MS.

Main findings: Studies using spICP-MS revealed the presence of the originally administrated Au NPs (40 nm diameter) and some evidences of other Au-containing species due to the increased background signal. Images obtained by transmission electron microscopy (TEM) showed the predominant presence of particles of significantly smaller diameter (6 ± 2 nm). As complementary method, HPLC-ICP-MS confirmed the presence of both particle types indicating a degradation of the Au NPs accompanied by detection of low-molecular Au species.

Conclusions: This study underlines that degradation of gold nanoparticles to low-molecular gold species might have to be taken into account in future for studies on their toxicological behaviour and their potential use in clinical applications.

1. Introduction

Since the industrial use of nanomaterials (NMs) has continuously grown in the last two decades, their impact on the environment and the biosphere is of general concern. Among them, Au NPs attracted great interest for their use in electronics, catalysis, and solar cells, but also in biomedical applications. The evaluation of potential impact of these emerging materials on organisms requires analytical techniques being capable of delivering information about the elemental composition, size, shape and concentration of the particles as well as the possible release of ionic species in the case of metal-based NMs [1–3].

The great interest in tracing NPs in environmental and biological systems has encouraged the development of various methods for the analysis of Au NPs; in particular, ICP-MS was found to be a very valuable tool in various applications. Besides hyphenated techniques like flow field-flow fractionation [4–6], liquid chromatography [7,8] and electrophoresis [9,10] coupled to ICP-MS, single particle ICP-MS (spICP-MS) turned out to be a powerful alternative thanks to its simplicity of operation, its rapidness and its potential to provide valuable species information (e.g. the presence of solubilized ions together with the NPs) [11,12].

All these techniques were combined with different extraction strategies to address the fate of NPs in various biological samples [13]. In these experiments, alkaline solubilization with tetramethylammonium hydroxide (TMAH) resulted in recoveries between 86 and 123% of 10 and 60 nm Au NPs as total Au. However, initial investigations using asymmetrical flow field-flow fractionation (AF4) on separating the Au NPs extracted this way (stabilized by bovine serum albumin) did not succeed [5]. TMAH extraction also turned out to be suitable for the analysis of Au and Ag NPs in ground beef using spICP-MS [14].

* Corresponding authors.
E-mail addresses: crissg@ugr.es (C. Sánchez-González), bettmerjorg@uniovi.es (J. Bettmer).

https://doi.org/10.1016/j.jtemb.2019.05.006
Received 25 February 2019; Received in revised form 29 April 2019; Accepted 9 May 2019

Loeschner et al. compared the use of alkaline (TMAH) and enzymatic (proteinase K) digestion for the determination of 60 nm Au NPs in Wistar rat spleen tissues after intravenous injection using spICP-MS [15]. This technique showed significant lower recovery of the sought species after enzymatic digestion due to inferior transport efficiency of Au NPs in the presence of enzymatically digested tissue residues. In another approach, tomato plant samples were analyzed by spICP-MS after releasing Au NPs enzymatically by Macerozyme R-10 enzyme [16]. Jenkins et al. studied spICP-MS for the discrimination of Au NPs and their agglomerates in spiked blood samples [17].

Lately, methods based on liquid chromatography coupled ICP-MS have become popular due their ability to distinguish between particle-bound metals and the corresponding low-molecular (ionic) species [18,19]. HeLA cells and cell media were analyzed after incubation with 10 nm Au NPs or dissolved Au^{3+} in order to follow their transformation in the different environment [20]. A similar study was conducted on the lysates of algae cells after incubation with 10 nm Au NPs or dissolved Au^{3+} [21]. Recently, our group studied the use of HPLC-ICP-MS for the analysis of 10 nm Au NPs (NIST RM 8011) in Wistar rat liver and spleen tissues after intraperitoneal injection [22]. By applying enzymatic solubilization with proteinase K, a remarkable fraction of total Au (˜ 30%) turned out to be present as ionic species indicating the importance of NP degradation processes during their transport, storage and metabolism in biological organisms. This type of Au NP degradation was also observed for other particle sizes [23].

Understanding the fate of Au NPs within biological systems is, therefore, of high importance, and analytical techniques are required to monitor the accumulation and potential degradation of the sought nanoparticles. In this study, we aim a comparative study of spICP-MS, HPLC-ICP-MS and TEM for tracing citrate-stabilized Au NPs in rat liver tissues after intraperitoneal injection. We intend to demonstrate that they can provide complementary data giving a more complete picture about the degradation and transformation of Au NPs in biological systems.

2. Materials and methods

2.1. Reagents and materials

All solutions were prepared using ultrapure water (> 18 MΩ cm) obtained from a MIlli-Q system (Millipore, Bedford, MA, USA). The investigated citrate-stabilised Au NPs of 40 nm nominal size in an aqueous suspension (GC-40) were obtained from Nanovex Biotechnologies S.L. (Llanera, Spain) and used without any further purification. Standard aqueous suspensions of citrate-stabilised Au NPs with nominal diameter of 10, and 30 nm (RM 8011, and 8012, respectively) were acquired from National Institute of Standards & Technology (NIST, Gaithersburg, MD, USA).

All tissue samples were prepared in phosphate-buffered saline (PBS). Sodium chloride was purchased from Prolabo (Leuven, Belgium) and potassium chloride, disodium hydrogen phosphate (Na_2HPO_4) and potassium dihydrogen phosphate (KH_2PO_4) were purchased from Merck (Darmstadt, Germany). In addition, tris(hydroxymethyl)aminomethane (TRIS, pH 7.5, Bio-Rad Laboratories, USA), sodium chloride (NaCl, ≥ 99%, Sigma-Aldrich), ethylenediaminetetraacetic acid disodium salt dihydrate (EDTA, Fluka) and TritonTM X-100 (Sigma-Aldrich) were used for the preparation of the lysis buffer. Sucrose (α-D-Glucopyranosyl, Sigma-Aldrich) was used for an additional pre-concentration step. The mobile phase for HPLC coupled to ICP-MS contained ammonium acetate (> 98%) adjusted to pH 6.8 and sodium dodecylsulfate (SDS, 98.5%) both from Sigma-Aldrich. For spICP-MS experiments, methanol (Fisher, Geel, Belgium) was used to dilute all the samples. Elemental standard solution of Au (1000 mg L^{-1}) was purchased from Merck. The ICP-MS was operated with Alphagaz Argon (purity 99.999%, Air Liquid, Valladolid, Spain) and was daily optimized in terms of detection sensitivity by introducing a multi-element tuning solution with a concentration of 1 µg L^{-1} of each element (Merck). $^{7}Li^{+}$, $^{89}Y^{+}$, $^{205}Tl^{+}$ were used for the sensitivity check, double-charged ions by measuring the ratio $^{140}Ce^{+}/^{140}Ce^{2+}$, and finally, the oxide formation was monitored by the ratio $^{140}Ce^{16}O^{+}/^{140}Ce^{+}$.

Table 1
Instrumental settings of the ICP-MS coupled to HPLC and in the single particle mode.

ICP-MS system	
Instrument	Agilent 7700
RF power	1500 W
Auxiliary gas flow	0.87 L·min^{-1}
Coolant gas flow	15.5 L·min^{-1}
Isotope monitored	^{197}Au
Dwell time	100 ms (HPLC)
	10 ms (spICP-MS)
Nebulizer	Meinhard type (HPLC)
	EnyaMist (spICP-MS)
Spray chamber (T)	Scott type (2 °C) (HPLC)
	Home-made total consumption spray chamber (spICP-MS) [22]
Nebulizer gas flow	1.1 L min^{-1} (HPLC)
	1.1 L min^{-1} (spICP-MS)
Sample flow rate	0.5 mL min^{-1} (HPLC)
	10 µL min^{-1} (spICP-MS)
HPLC system	
Instrument	Shimadzu LC-10AD
Column	Nucleosil 7 µm particle size, C18, 1000 Å pore size, 250 x 4.6 mm ID
Mobile phase	10 mmol L^{-1} ammonium acetate, 10 mmol L^{-1} SDS, pH 6.8
Injection volume	20 µL

2.2. Instrumentation

All measurements were performed using the quadrupole based inductively coupled plasma mass spectrometer (ICP-MS) Agilent 7700 (Agilent Technologies, Tokyo, Japan). Chromatographic separations were carried out on a Nucleosil C18 column (Phenomenex, Aschaffenburg, Germany) with an HPLC pump (LC-10AD, Shimadzu Corporation, Kyoto, Japan) and a 6-way injection valve (Rheodyne model 3125, Cotati, CA, USA). All connections and the injection loop (20 µL) were made of PEEK. The coupling was realized by directly connecting the column outlet to the nebulizer of the ICP-MS instrument at a flow rate of 0.5 mL min^{-1}. Detailed information are summarized in Table 1. For the single particle experiments, the ICP-MS was equipped with a micro nebulizer, EnyaMist (ESI Elemental Service & Instruments GmbH, Mainz, Germany) operated at a flow rate of 10 µL·min^{-1} using an syringe pump (SP100IZ syringe pump, World Precision Instruments, Sarasota, FL, USA) and a home-made total consumption spray chamber [24]. A dwell time of 10 ms was chosen ($^{197}Au^{+}$). The ICP-MS was used in time-resolved analysis (TRA) mode and the acquisition time of each run was typically 180 s. For the further characterization of Au NPs in the tissues, a high resolution transmission electron microscope JEOL JEM 2000ExII (Jeol Ltd, Tokyo, Japan) was used.

2.3. Sample preparation

Animals. Two adult male Wistar rats (180–200 g of weight) were purchased from Charles River Laboratories (L'Arbresle, France). Citrate-stabilized gold nanoparticles suspension (40 nm) was injected intraperitoneally at a single dose to the first rat (2 mL of 50 µg mL^{-1}). The second rat was injected with 2 mL of ultrapure water.

After 4 h of formulation administration, both rats were anesthetized with a solution of ketamine (0.75 mg kg^{-1} body weight) and xylazine (0.10 mg kg^{-1} body weight) (both from Fatro Ibérica, Barcelona, Spain), and exsanguinated by cannulating the posterior aorta. Each liver was removed, weighed, placed in pre-weighed polyethylene vials, and stored at −80 °C until analysis.

All experiments with rats were carried out in accordance with Directional Guides Related to Animal Housing and Care and all procedures were approved by the Animal Experimentation Ethics Committee of the University of Granada.

NP extraction. Liver was excised in little portions, snap frozen and homogenised in a mortar cooled with liquid nitrogen to grind and pulverize samples. The resulting frozen liver powder from each sample were suspended into the appropriate volume of cold lysis buffer (containing 150 mmol·L^{-1} NaCl, 1 mmol·L^{-1} EDTA, 20 mmol·L^{-1} Tris-HCl (pH 7.5), 1% (v/v) Triton X-100). This suspension underwent sonication in an ice bath for 15 min. Lysates were cleared by centrifugation for 15 min at 13,000*g* and 4 °C and were further used for TEM, spICP-MS and HPLC-ICP-MS studies.

3. Results and discussion

The purpose of applying different techniques was the determination of particle sizes and size distribution by spICP-MS and the detection of eventually present smaller nanoparticles (< 18 nm that was the size detection limit of spICP-MS) and their corresponding low-molecular Au species by HPLC-ICP-MS. In order to visualize the particles, TEM was applied as a complementary technique. The nominal size given by the producer was 40 nm and was determined to be (37 ± 2) nm by our TEM measurements (Fig. S1).

First, the EnyaMist nebulizer was tested for spICP-MS analysis as it showed recently excellent suitability for single cell analysis [24]. This nebulizer was chosen due to the expected higher transport efficiency in comparison to standard pneumatic nebulizers accompanied by a reduction of sample consumption. The sample flow was fixed to 10 µL min^{-1}. According to the manufacturer the addition of an organic modifier was recommended. The variation of the methanol concentration between 0 and 15% (v/v) showed that pure suspensions of 30 nm Au NPs in water resulted in a relatively unstable aerosol with significantly lower transport efficiency and detection sensitivity (Fig. 1). A maximum transport efficiency was obtained at methanol concentrations of 10% (v/v). Increasing methanol concentrations resulted in higher sensitivity of the individual particle pulses. However, in order to prevent carbon deposition on the sampler cone, it was decided to continue further studies with 10% methanol.

Under these conditions, the transport efficiency was determined by relating the pulse frequency to the calculated particle number concentration of the NIST materials [11,25] and determined to be 48.3% for the 30 nm Au NPs. Using these parameters for spICP-MS analysis, the 40 nm Au NPs suspension was characterized in terms of size and distribution. The corresponding spICP-MS experiment and the particle size distribution can be found in Fig. S2. The obtained average particle size ((34 ± 5) nm) was in good agreement with the TEM data (37 ± 2 nm). and served as a reference for the following studies. They

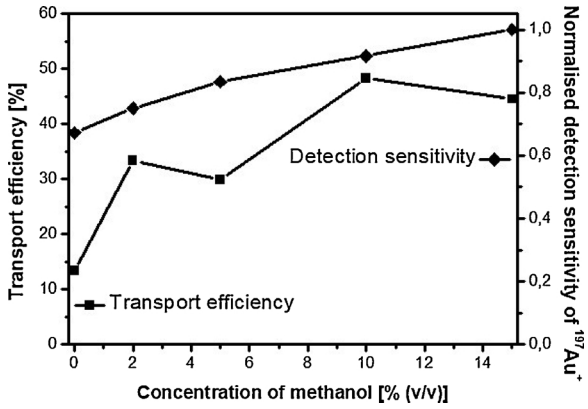

Fig. 1. Influence of the methanol concentration on the detection sensitivity and transport efficiency.

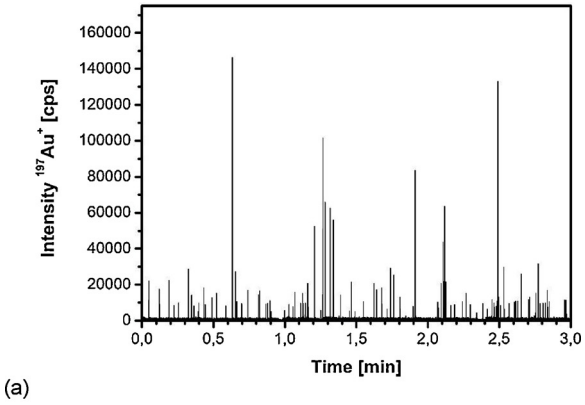

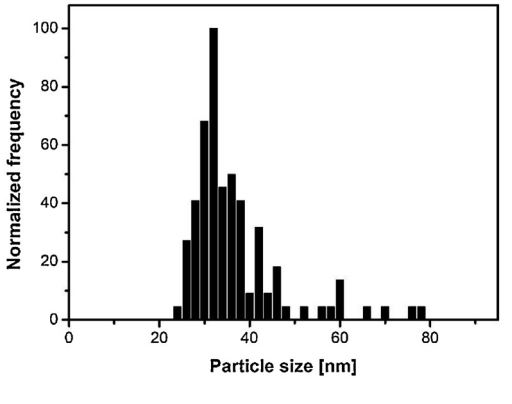

Fig. 2. Analysis of Au NPs in the extract of a rat liver tissue by spICP-MS. (a) Time-resolved measurement of Au, and (b) the resulting size distribution (bin size: 2 nm).

had the aim to investigate and determine the potential degradation of Au NPs in biological systems.

The 40 nm Au NPs suspension was injected intraperitoneally into a Wistar rat and the liver tissue was prepared for further analysis as described in the experimental section. The lysate of the liver tissue was diluted 1:20 in a methanol/water mixture (10/90, v/v) and analysed by spICP-MS. No significant matrix effects on the detection sensitivity were found. Fig. 2 illustrates the obtained time-resolved measurement (Fig. 2a) and the resulting particle size distribution (Fig. 2b). The particle size distribution was equal to the one of the standard suspension (Fig. S2) indicating the adequate performance of the whole strategy to preserve the originally injected Au NPs. The background was slightly higher than in the spICP-MS experiments of the standard. The background signal increased from approximately 100 cps to 1000 cps. This observation suggested the presence of dissolved Au species or Au NPs of a size smaller than the achievable (size) detection limits (˜18 nm using the 3σ-criterion [12]) and indicated a degradation of the originally administrated nanoparticles. Such a degradation in biological systems was also observed in other studies, e.g. for Ag NPs after oral administration in rats [26] or for Au NPs after intraperitoneal injection [22].

In order to prove the findings, complementary TEM measurements should reveal the presence of the initially administrated Au NPs and other potentially present NPs of smaller diameter. Fig. 3 depicts a TEM image of the previously analysed lysate solution. As can be observed, various NPs were present with an average diameter of (6 ± 2) nm. In contradiction to the spICP-MS analysis, the Au NPs of original size (37 ± 2 nm) could not be observed. According to the spICP-MS and the TEM measurements, the detected number of bigger sized NPs was quite low or even negligible. Interestingly, the size distribution of the

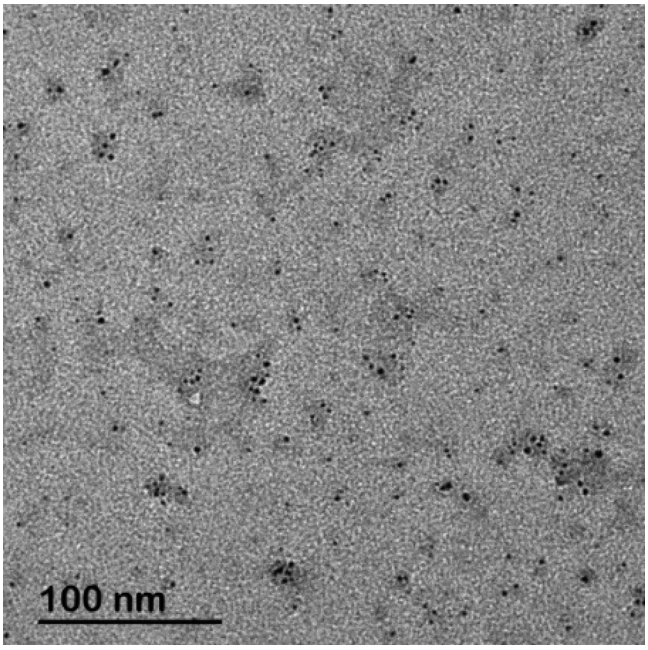

Fig. 3. TEM image of the extracted Au NPs from the liver tissue.

observed particle sizes in the TEM images is relatively narrow. As the observed population of smaller particles presented sizes below the detection limit of spICP-MS, the latter method only revealed the presence of bigger Au NPs. On the other hand, the TEM image gave a first proof that smaller particles were predominantly accumulated in the liver tissue, probably due to degradation during transport and/or accumulation in the tissue.

Since HPLC-ICP-MS has proven to be a versatile tool for the analysis of Au and Ag NPs in a size range between roughtly 2 and 50 nm and their corresponding ionic species [7,9,27], this was the next strategy to be tested. In combination with an enzymatic extraction (proteinase K), it provided important information about different Au species (NPs and ionic species) present in rat liver tissues [22,23].

Thus, the previously obtained lysate was subjected after 1:10 dilution in the mobile phase to this complementary method. The presence of SDS in the mobile phase was necessary to elute nanoparticles from the column [7]. It should also facilitate protein denaturation and reduce the protein corona formed around the nanoparticles. A representative chromatogram is shown in Fig. 4. Three different fraction could be observed, each one with very low abundance. A relatively broad NP fraction eluted between 3.5 and 4.5 min) and could be correlated to Au NPs with sizes of around 30 nm (NIST 8012 (30 nm Au NPs) elute at 3.9 min). Obviously, they represent the particles initially administrated and beforehand detected by the spICP-MS experiments. The second fraction between 4.5 and 5 min reflected the presence of smaller Au NPs (roughly between 6 and 10 nm, NIST 8011 (10 nm Au NPs) eluted at 4.6 min.) in agreement with the observation in the TEM measurements.

Comparing the peak areas of both fractions resulted in a ratio of approximately 2:1 (fraction 1 : fraction 2). This is, at first view, contradictory to the observation by TEM in which the fraction of smaller Au NPs was dominant. In order to explain this result, it has to be kept in mind that each particle of the fraction containing the bigger Au NPs (˜37 nm diameter) consists of about 200 times more Au atoms than the particles of the smaller size (˜6 nm)[1] . This means that equal particle number concentrations would result in a roughly 200 times larger peak area for the bigger Au NPs. In conclusion, the observed peak intensity

[1] For spherical particles with a volume (V) and diameter (d) following $V = \frac{1}{6}\pi d^3$.

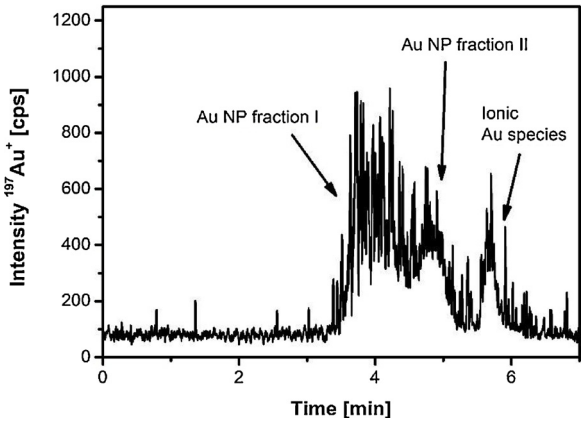

Fig. 4. Chromatogram of the liver lysate after dilution in the mobile phase (1:10, v/v).

for the fraction of the smaller Au NPs revealed a clearly higher particle number concentration. The third peak proved the presence of low-molecular Au species that obviously appeared due to particle degradation. In fact, TEM is not capable of monitoring these species. Thus, the HPLC-ICP-MS approach revealed the presence of two differently sized NP fractions, and additionally, low-molecular species. Other studies reported about the presence of such Au species in different biological systems [18,20–22] and their presence should be taken into consideration for any toxicological study [28].

These studies clearly revealed that the administrated Au NPs were predominantly degraded to smaller ones of a narrow size distribution. Although the mechanism remains unclear, the significant reduction in size might accompanied by a reduced cytotoxicity of Au NPs [28]. Sulphur-containing compounds like cysteine have been recognized for its influence on the dissolution of Ag NPs [29] and could play a significant role for the observed effects on Au NPs. As “side effect”, low-molecular Au species were formed, but it could not be clarified whether the processes appeared during the transport and/or accumulation of the Au NPs.

4. Conclusions

The stability of citrate-coated Au NPs was investigated in liver samples after intraperitoneal injection into Wistar rats. The application of three different techniques (spICP-MS, TEM, and HPLC-ICP-MS) revealed the presence of the originally administrated Au NPs with a diameter of approximately 37 nm together with nanoparticles with a significantly smaller size (6 ± 2 nm). The latter ones could be only detected by TEM and HPLC-ICP-MS as their sizes were lower than the size detection limit obtainable by spICP-MS. Another product of the observed degradation process, low-molecular Au species, could be detected by HPLC-ICP-MS. These findings underlined that the monitoring of the fate of nanoparticles in biological systems requires various complementary techniques in order to fully understand the evolution of the sought species. Although little is known about the mechanism of nanoparticle degradation within a biological system, the detection of particles with significantly smaller diameters and the corresponding low-molecular species (in this case of Au) might help to understand the defence mechanisms of living organisms to the exposure of nanomaterials.

Author contributions

C. S.-G., J. L., M. M.-B. and J. B. conceived and designed the experiments; R. A.-F.G., N. F.-I. and C. L.-C. performed the experiments; all authors analyzed the data; J. B. wrote the paper.

Conflicts of interest

The authors declare no conflict of interest.

Acknowledgements

The authors gratefully acknowledge the financial support from the Spanish MICINN (Spanish ministry for science and innovation, Grant Numbers CTQ2011-23038 and MINECO-16-CTQ2015-69583-R), from the FICYT (Grant number: FC-15-GRUPIN14-010) and MECD (Spanish ministry for education culture and sports, Grant Number FPU13/00062). R. Álvarez-Fernández García acknowledges his fellowship from FINBA (Foundation for Biosanitary Research and Innovation of the Government of Asturias).

Appendix A. Supplementary data

Supplementary material related to this article can be found, in the online version, at doi:https://doi.org/10.1016/j.jtemb.2019.05.006.

References

[1] S. Sharifi, S. Behzadi, S. Laurent, M.L. Forrest, P. Stroeve, M. Mahmoudi, Toxicity of nanomaterials, Chem. Soc. Rev. 41 (2012) 2323–2343, https://doi.org/10.1039/C1CS15188F.
[2] T.M. Benn, P. Westerhoff, Nanoparticle silver released into water from commercially available sock fabrics, Environ. Sci. Technol. 42 (2008) 4133–4139, https://doi.org/10.1021/es7032718.
[3] SO/TS 19590, Nanotechnologies – Size Distribution and Concentration of Inorganic Nanoparticles in Aqueous Media via Single Particle Inductively Coupled Plasma Mass Spectrometry, (2017).
[4] H. Hagendorfer, R. Kaegi, J. Traber, S.F.L. Mertens, R. Scherrers, C. Ludwig, A. Ulrich, Application of an asymmetric flow field flow fractionation multi-detector approach for metallic engineered nanoparticle characterization – prospects and limitations demonstrated on Au nanoparticles, Anal. Chim. Acta 706 (2011) 367–378, https://doi.org/10.1016/j.aca.2011.08.014.
[5] B. Schmidt, K. Loeschner, N. Hadrup, A. Mortensen, J.J. Sloth, C. Bender Koch, E.H. Larsen, Quantitative characterization of gold nanoparticles by field-flow fractionation coupled online with light scattering detection and inductively coupled plasma mass spectrometry, Anal. Chem. 83 (2011) 2461–2468, https://doi.org/10.1021/ac102545e.
[6] S. López-Sanz, N. Rodríguez Fariñas, Rd.C. Rodríguez Martín-Doimeadios, A. Rios, Analytical strategy based on asymmetric flow field flow fractionation hyphenated to ICP-MS and complementary techniques to study gold nanoparticles transformations in cell culture medium, Anal. Chim. Acta 1053 (2019) 178–185, https://doi.org/10.1016/j.aca.2018.11.
[7] A. Helfrich, W. Brüchert, J. Bettmer, Size characterisation of Au nanoparticles by ICP-MS coupling techniques, J. Anal. At. Spectrom. 21 (2006) 431–434, https://doi.org/10.1039/B511705D.
[8] E.P. Gray, T.A. Bruton, C.P. Higgins, R.U. Halden, P. Westerhoff, J.F. Ranville, Analysis of gold nanoparticle mixtures: a comparison of hydrodynamic chromatography (HDC) and asymmetrical flow field-flow fractionation (AF4) coupled to ICP-MS, J. Anal. At. Spectrom. 27 (2012) 1532–1539, https://doi.org/10.1039/C2JA30069A.
[9] A. Helfrich, J. Bettmer, Analysis of gold nanoparticles using ICP-MS-based hyphenated and complementary ESI-MS techniques, Int. J. Mass Spectrom. 307 (2011) 92–98, https://doi.org/10.1016/j.ijms.2011.01.010.
[10] B. Franze, C. Engelhard, Fast Separation, characterization, and speciation of gold and silver nanoparticles and their ionic counterparts with micellar electrokinetic chromatography coupled to ICP-MS, Anal. Chem. 86 (2014) 5713–5720, https://doi.org/10.1021/ac403998e.
[11] C. Degueldre, P.-Y. Favarger, S. Wold, Gold colloid analysis by inductively coupled plasma-mass spectrometry in a single particle mode, Anal. Chim. Acta 555 (2006) 263–268, https://doi.org/10.1016/j.aca.2005.09.021.
[12] F. Laborda, E. Bolea, J. Jiménez-Lamana, Single particle inductively coupled plasma mass spectrometry: a powerful tool for nanoanalysis, Anal. Chem. 86 (2014) 2270–2278, https://doi.org/10.1021/ac402980q.
[13] C.-K. Su, Y.-C. Sun, Considerations of inductively coupled plasma mass spectrometry techniques for characterizing the dissolution of metal-based nanomaterials in biological tissues, J. Anal. At. Spectrom. 30 (2015) 1689–1705, https://doi.org/10.1039/C5JA00132C.
[14] E.P. Gray, J.G. Coleman, A.J. Bednar, A.J. Kennedy, J.F. Ranville, C.P. Higgins, Extraction and analysis of silver and gold nanoparticles from biological tissues using single particle inductively coupled plasma mass spectrometry, Environ. Sci. Technol. 47 (2013) 14315–14323, https://doi.org/10.1021/es403558c.
[15] K. Loeschner, M.S.J. Brabrand, J.J. Sloth, E.H. Larsen, Use of alkaline or enzymatic sample pretreatment prior to characterization of gold nanoparticles in animal tissue by single-particle ICPMS, Anal. Bioanal. Chem. 406 (2014) 3845–3851, https://doi.org/10.1007/s00216-013-7431-y.
[16] Y. Dan, W. Zhang, R. Xue, X. Ma, C. Stephan, H. Shi, Characterization of gold nanoparticle uptake by tomato plants using enzymatic extraction followed by single-particle inductively coupled plasma–mass spectrometry analysis, Environ. Sci. Technol. 49 (2015) 3007–3014, https://doi.org/10.1021/es506179e.
[17] S.V. Jenkins, H. Qu, T. Mudalige, T.M. Ingle, R. Wang, F. Wang, P.C. Howard, J. Chen, Y. Zhang, Rapid determination of plasmonic nanoparticle agglomeration status in blood, Biomaterials 51 (2015) 226–237, https://doi.org/10.1016/j.biomaterials.2015.01.072.
[18] Y. Yang, L. Luo, H.-P. Li, Q. Wang, Z.-G. Yang, Z.-P. Qu, R. Ding, Analysis of metallic nanoparticles and their ionic counterparts in complex matrix by reversed-phase liquid chromatography coupled to ICP-MS, Talanta 182 (2018) 156–163, https://doi.org/10.1016/j.talanta.2018.01.077.
[19] J. García Fernández, C. Sánchez-González, J. Bettmer, J. Llopis, N. Jakubowski, U. Panne, M. Montes-Bayón, Quantitative assessment of the metabolic products of iron oxide nanoparticles to be used as iron supplements in cell cultures, Anal. Chim. Acta 1039 (2018) 24–30, https://doi.org/10.1016/j.aca.2018.08.003.
[20] S. López-Sanz, N. Rodríguez-Fariñas, R. Serrano Vargas, R.D.C. Rodríguez Martín-Doimeadios, A. Ríos, Methodology for monitoring gold nanoparticles and dissolved gold species in culture medium and cells used for nanotoxicity tests by liquid chromatography hyphenated to inductively coupled plasma-mass spectrometry, Talanta 164 (2017) 451–457, https://doi.org/10.1016/j.talanta.2016.11.060.
[21] J. Malejko, N. Swierzewska, A. Bajguz, B. Godlewska-Zylkiewicz, Method development for speciation analysis of nanoparticle and ionic forms of gold in biological samples by high performance liquid chromatography hyphenated to inductively coupled plasma mass spectrometry, Spectrochim. Acta B 142 (2018) 1–7, https://doi.org/10.1016/j.sab.2018.01.014.
[22] J. Soto-Alvaredo, C. López Chaves, C. Sánchez-González, M. Montes-Bayón, J. Llopis, J. Bettmer, Speciation of gold nanoparticles and low-molecular gold species in Wistar rat tissues by HPLC coupled to ICP-MS, J. Anal. At. Spectrom. 32 (2017) 193–199, https://doi.org/10.1039/C6JA00248J.
[23] C. Lopez-Chaves, J. Soto-Alvaredo, M. Montes-Bayon, J. Bettmer, J. Llopis, C. Sanchez-Gonzalez, Gold nanoparticles: distribution, bioaccumulation and toxicity. In vitro and in vivo studies, Nanomed. Nanotechnol. Biol. Med. 14 (2018) 1–12, https://doi.org/10.1016/j.nano.2017.08.011.
[24] M. Corte Rodríguez, R. Álvarez-Fernández García, E. Blanco, J. Bettmer, M. Montes-Bayón, Quantitative evaluation of cisplatin uptake in sensitive and resistant individual cells by single-cell ICP-MS (SC-ICP-MS), Anal. Chem. 89 (2017) 11491–11497, https://doi.org/10.1021/acs.analchem.7b02746.
[25] H.E. Pace, N.J. Rogers, C. Jarolimek, V.A. Coleman, C.P. Higgins, J.F. Ranville, Determining transport efficiency for the purpose of counting and sizing nanoparticles via single particle inductively coupled plasma mass spectrometry, Anal. Chem. 83 (2011) 9361–9369, https://doi.org/10.1021/ac201952t.
[26] K. Loeschner, N. Hadrup, K. Qvortrup, A. Larsen, X. Gao, U. Vogel, A. Mortensen, H. Rye Lam, E.H. Larsen, Distribution of silver in rats following 28 days of repeated oral exposure to silver nanoparticles or silver acetate, Part. Fibre Toxicol. 8 (2011) 18, https://doi.org/10.1186/1743-8977-8-18.
[27] C.A. Sötebier, S.M. Weidner, N. Jakubowski, U. Panne, J. Bettmer, Separation and quantification of silver nanoparticles and silver ions using reversed phase high performance liquid chromatography coupled to inductively coupled plasma mass spectrometry in combination with isotope dilution analysis, J. Chromatogr. A 1468 (2016) 102–108, https://doi.org/10.1016/j.chroma.2016.09.028.
[28] S.K. Misra, A. Dybowska, D. Berhanu, S.N. Luoma, E. Valsami-Jones, The complexity of nanoparticle dissolution and its importance in nanotoxicological studies, Sci. Total Environ. 438 (2012) 225–232, https://doi.org/10.1016/j.scitotenv.2012.08.066.
[29] A.P. Gondikas, A. Morris, B.C. Reinsch, S.M. Marinakos, G.V. Lowry, H. Hsu-Kim, Cysteine-induced modifications of zero-valent silver nanomaterials: implications for particle surface chemistry, aggregation, dissolution, and silver speciation, Environ. Sci. Technol. 46 (2012) 7037–7045, https://doi.org/10.1021/es3001757.